



1 **Evaporation, infiltration and storage of soil water in**
2 **different vegetation zones in Qilian mountains: From**
3 **a perspective of stable isotopes**

4 Guofeng Zhu ^{a,b*}, Leilei Yong ^{a,b}, Zhao Xi ^{a,b}, Yuwei Liu ^{a,b}, Zhuangxia Zhang ^{a,b}, Yuanxiao Xu ^{a,b},
5 Zhigang Sun ^{a,b}, Liyuan Sang ^{a,b}, Lei Wang ^{a,b}

6 ^a *College of Geography and Environment Science, Northwest Normal University, Lanzhou*
7 *730070, China*

8 ^b *Shiyang River Ecological Environment Observation Station, Northwest Normal University,*
9 *Lanzhou 730070, Gansu, China*

10 *Correspondence to: Guofeng Zhu (zhugf@nwnu.edu.cn)*

11 **Abstract:** In arid areas, almost all the water resources in the basin come from
12 mountainous areas. Nevertheless, the process of water storage and runoff generation
13 has not been fully understood in different vegetation zones in mountainous areas,
14 which is the main obstacle blocking human cognition of hydrological processes and
15 water resources assessment. In current study, the spatiotemporal dynamics of stable
16 isotopes were monitored in different water bodies and soil water storage in different
17 vegetation zones in the upper reaches of Xiyang River. The results show that: (1) The
18 water storage capacity of surface soil was weak in vegetation zones, and soil water
19 was mainly saved up in the middle and lower soil layers. (2) Surface and subsurface
20 runoff could form in the Alpine Meadow and Coniferous Forest during the rainy
21 season and the snow melting season. The lower elevation vegetation zones of
22 Mountain Grassland and Deciduous forest evaporate strongly and infiltrate partially
23 into the middle and bottom layers of the soil to store or recharge groundwater, rarely
24 generating surface runoff. This work would provide a scientific foundation for
25 reasonably explaining the mechanism of water production in mountainous areas of
26 arid regions, and provide a reference for formulating management policies suitable for
27 sustainable development of water resources and improving the ability to cope with
28 climate change in arid areas.



29 **Key words:** Xiying River; Stable isotope; Drought, Soil water storage

30 **1. Introduction**

31 In arid inland river basins, climate change and distribution of water resources in
32 different vegetation zones restrict the sustainable development of the regional
33 ecological environment (Wang et al., 2012; Tetzlaff et al., 2013). To cope with
34 the changing natural environment, managers have formulated a series of scientific
35 ecological governance policies based on species selection (Wookey et al., 2010),
36 crop rotation (Zhu et al., 2019), and ecological water conveyance (Zhang et al.,
37 2019), which has been improving their adaptability to the evolving natural
38 environment.

39 Unsaturated soil zone is the center of transforming natural precipitation into
40 water vapor, soil water storage, and groundwater recharge. Its evaporation, infiltration,
41 and water storage are very critical for understanding the regional hydrological process
42 and water balance under the background of climate and vegetation changes (Brooks
43 et al., 2010; Grant and Dietrich, 2017). Isotopes, as "fingerprints" of water, have
44 been used to trace eco-hydrological processes such as evaporation (Barnes and
45 Allison, 1988), groundwater recharge (Koeniger et al., 2016), infiltration path
46 (Tang and Feng, 2004), evapotranspiration distribution (Xiao et al., 2018) and
47 water absorption by plants (Rothfuss and Javaux, 2017).

48 Evaporation, infiltration, and storage are the main forms of soil water transport
49 after precipitation input. After a rainfall, the dynamic fractionation caused by
50 evaporation makes soil water isotopes enriched on the surface (Ferretti et al., 2003).
51 Affected by air temperature and precipitation, soil moisture fractionation is positively
52 correlated with evapotranspiration but negatively correlated with precipitation (Hsieh
53 et al., 1998). Therefore, compared with autumn and winter, the isotope composition
54 of soil profiles is quite different in spring and summer (Barberta et al., 2015), and
55 the difference is more significant in lower altitude areas than in higher altitude areas
56 (Cui et al., 2009). In addition, vegetation and topography will also affect the
57 dynamic fractionation of soil water, and the increase of vegetation coverage will



58 weaken the evaporation of soil water (Dubbert et al., 2013). The d-excess on
59 hillsides were lower than in summer valleys(Simonin et al., 2014). Seasonal
60 variation of precipitation isotopes is often used to track the seepage process in moist
61 soil (Stumpp et al., 2012). Before soil water reaches the saturation zone, the
62 seasonal variation of the input water isotopic signal is usually highly attenuated
63 (Sprenger et al., 2017). High variability of isotope ~~signal~~ in the soil profile and
64 seasonal lack of precipitation signal can identify a preferential flow in soil
65 (Peralta-Tapia et al., 2015). The cyclic change of isotope composition reflects new
66 water transfer to old water (Sprenger et al., 2016a). It is found that most seepage
67 processes are the result of the interaction of plug flow and macropore preferential
68 flow (Cheng et al., 2014), and which infiltration mode plays a leading role depends
69 on soil structure, soil texture, precipitation intensity, and soil humidity (Wenner et
70 al., 1991; Seiler et al., 2002). After evaporation and seepage processes, some water
71 will be stored in the soil. Generally speaking, the water storage capacity of wet areas
72 is higher than that of arid areas, the water storage capacity of forests is higher than
73 that of grassland, and the water storage capacity of middle and lower soil layers with
74 higher clay content is higher than surface soil layer (Kleine et al., 2020; Heinrich
75 et al., 2019; Sprenger et al., 2019).

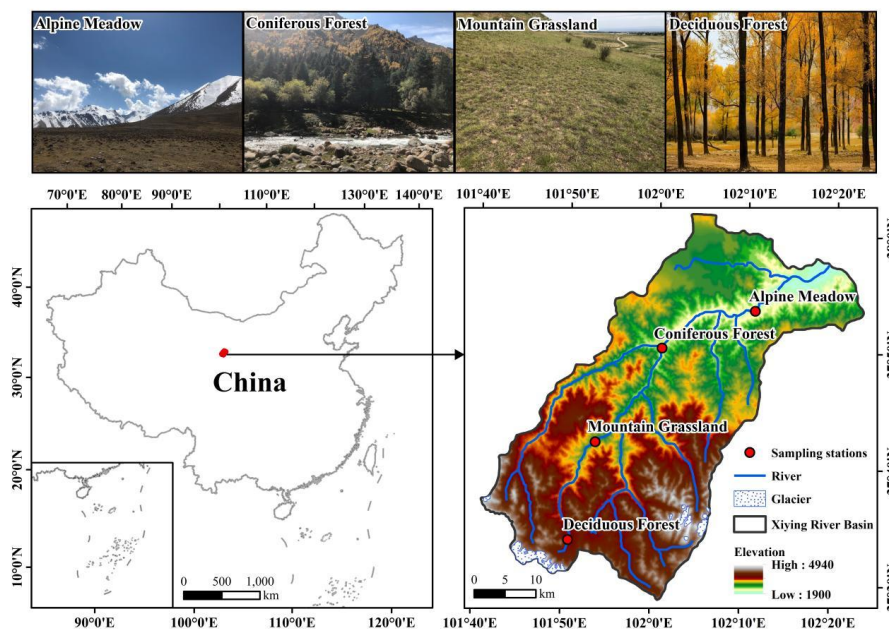
76 In the future, climate warming will force water resources to become more
77 unstable, and the dynamic interaction between water bodies stored in different media
78 will become the main focus in the process of water circulation (Penna et al., 2018).
79 Understanding the climatic and hydrological conditions of different vegetation zones
80 and clarifying the regulating role of vegetation in the water cycle process can better
81 adapt to the impact of climate change on the hydrological process in arid headwaters.
82 In current study, the stable isotopic composition of precipitation and soil water and
83 soil water storage's spatiotemporal dynamics were monitored in four vegetation zones
84 with different water and heat conditions in the Xiyang River Basin. In order to explore
85 the similarities and differences of soil water evaporation, infiltration and storage, we
86 put forward the following research objectives: (1) Evaluate the soil water storage



87 capacity and its influencing factors in different vegetation zones in the basin; (2)
88 Explore the evolution of isotopic evaporation signal and the "memory" effect of
89 precipitation input, mixing and rewetting; (3) Analyze the mechanism of runoff
90 generation and water storage in different vegetation zones.

91 **2. Study area**

92 Xiyang River originates from Lenglongling and Kawazhang in the eastern Qilian
93 Mountains ($101^{\circ}40'47''\sim 102^{\circ}23'5''E, 37^{\circ}28'22''\sim 38^{\circ}1'42''N$) (Fig.1). As the
94 largest first-class tributary of Shiyang River, it is formed by Shuiguan River,
95 Ningchang River, Xiangshui River and, Tatu River converging from southwest to
96 northeast, and finally flowing into Xiyang Reservoir. The annual runoff of the Xiyang
97 River is 388 million cubic meters, which is mainly replenished by mountainous
98 precipitation and melting water of ice and snow. The runoff is concentrated primarily
99 in summer. The altitude of the basin is about 2000-5000m, which belongs to a
100 continental temperate arid climate with strong solar radiation, long sunshine time, and
101 large temperature difference between day and night. The annual rainfall is between
102 300 mm and 600 mm, and the annual evaporation is between 700 mm and 1200 mm.
103 The zonal differentiation of vegetation in the basin is dominated by temperate
104 Deciduous Forest, Mountain Grassland, Cold Temperate Coniferous Forest, and
105 Alpine Meadow. The soils are mainly lime soil, chestnut soil, alpine shrub meadow
106 soil, and desert soil.



107
108

Fig. 1 Study area and location of sampling points

109 **3. Data and methods**

110 **3.1 Sample collection and determination**

111 In this study, soil water and precipitation samples were collected from April to
112 October 2017 (plant growing season) in four vegetation zones in Xiyang River Basin
113 (Table 1).

114 Collection of soil samples: Soil samples were collected once a month at depths
115 of 0-10, 10-20, 20-30, 30-40, 40-50, 50-60, 60-70, 70-80, 80-90, and 90-100 cm from
116 soil layers in four vegetation zones. Also, four parallel samples for each soil layer
117 were collected and performed the following operations: put three of them into a 50
118 mL glass bottle, sealed the bottle with Parafilm, wrote down the sampling date and
119 depth on the bottle, then frozen and stored until experimental isotopic analysis, and
120 another parallel sample placed in an aluminum box, weighed and documented, and
121 stored until an experimental analysis of soil moisture content, overall soil bulk density,
122 etc.

123 Collection of precipitation samples: The precipitation samples were collected by



124 a plastic funnel bottle device. After each precipitation event, the collected
125 precipitation samples were immediately transferred to an 80 mL high-density
126 polyethylene bottle, and the bottle mouth of the samples was sealed with Parafilm
127 film, and then frozen and stored until the experimental analysis.

128 Meteorological data: During the sampling period, the local meteorological data
129 were obtained and recorded by the automatic weather stations (watchdog 2000 series
130 weather stations) erected near the sample plot.

131 **Table 1** Basic data of each Vegetation zone (*Long*-Longitude, *Lat*-Latitude, *Alt*-Altitude, *T*-Air
132 Temperature, *P*-Precipitation Amount, *h*-Relative Humidity)

Vegetation zone	Geographical parameter			Meteorological parameters			Number of samples	
	<i>Long</i> (°E)	<i>Lat</i> (°N)	<i>Alt</i> (m)	<i>T</i> (°C)	<i>P</i> (mm)	<i>h</i> (%)	Precipitation	Soil
Alpine Meadow	101°51'16"	37°33'28"	3637	-0.19	595.1	69.2	72	47
Coniferous Forest	101°53'23"	37°41'50"	2721	3.34	431.9	66.6	42	41
Mountain Grassland	102°00'25"	37°50'23"	2390	6.6	363.5	60.4	37	54
Deciduous Forest	102°10'56"	37°53'27"	2097	7.9	262.5	59.8	40	53

133 3.2 Sample determination

134 The analysis of $\delta^2\text{H}$ and $\delta^{18}\text{O}$ values of all the above water samples was
135 completed using a liquid water isotope analyzer (DLT-100, Los Gatos Research, USA)
136 in the stable isotope laboratory of Northwest Normal University. Before analyzing the
137 isotope values of soil water, the soil water should be extracted from the collected soil
138 samples by a low temperature vacuum condensation system (LI-2100, LICA United
139 Technology Limited, China). During the analysis, both water sample and isotope
140 standard sample were continuously injected 6 times. In order to avoid the memory
141 effect of isotope analysis, we discarded the first two injection values, used the average
142 value of the last four times as the final value. The analysis results were expressed in
143 thousandths of the Vienna Standard Mean Ocean Water (VSMOW):

$$\delta = \left(\frac{R_{\text{sample}}}{R_{\text{standard}}} - 1 \right) \times 1000\text{‰} \quad (1)$$



144 Where the R_{sample} is the ratio of $^{18}\text{O}/^{16}\text{O}$ or $^2\text{H}/^1\text{H}$ in the sample, and the $R_{standard}$ is the
145 ratio of $^{18}\text{O}/^{16}\text{O}$ or $^2\text{H}/^1\text{H}$ in VSMOW. The test error of $\delta^2\text{H}$ value does not exceed
146 $\pm 0.6\text{‰}$, and the test error of $\delta^{18}\text{O}$ value does not exceed $\pm 0.2\text{‰}$.

147 3.3 Analysis method

148 3.3.1 lc-excess

149 The linear relationship between $\delta^2\text{H}$ and $\delta^{18}\text{O}$ in precipitation and soil water is
150 defined as LMWL and SWL, respectively, which is of great significance for studying
151 evaporation fractionation of stable isotopes in the water cycle. Lc-excess in different
152 water bodies can characterize the evaporation of different water bodies relative to
153 local precipitation (Landwehr and Coplen, 2004).

$$\text{lc-excess} = \delta^2\text{H} - a \times \delta^{18}\text{O} - b \quad (2)$$

154 where a and b are the slope and intercept of LMWL, respectively, and $\delta^2\text{H}$ and $\delta^{18}\text{O}$
155 are the isotopic values of hydrogen and oxygen in the sample. The physical meaning
156 of lc-excess is expressed as the deviation degree between isotopic values in samples
157 and LMWL, which indicates the non-equilibrium dynamic fractionation process
158 caused by evaporation (Landwehr et al., 2014; Sprenger et al., 2017).

159 3.3.2 PET

160 Calculation of potential evapotranspiration based on Penman-Monteath equation
161 (Allen et al., 1998):

$$\text{PET} = \frac{0.408\Delta(R_n - G) + \gamma \frac{900}{T + 273} u^2 (e_s - e_a)}{\Delta + \gamma(1 + 0.34u^2)} \quad (3)$$

162 where PET is the daily potential evapotranspiration (mm day^{-1}), R_n is net radiation
163 ($\text{MJ m}^{-2} \text{day}^{-1}$), G is soil heat flux density ($\text{MJ m}^{-2} \text{day}^{-1}$), γ is humidity constant
164 ($\text{kPa}^\circ\text{C}^{-1}$), u_2 is the wind speed at a height of 2 m (m s^{-1}), T is the daily average
165 temperature ($^\circ\text{C}$), Δ is the slope vapor pressure curve ($\text{kPa}^\circ\text{C}^{-1}$), e_a is the actual steam
166 pressure (kPa) and e_s is saturated vapor pressure (kPa).

167 3.3.3 Soil water storage

168 Soil water storage is the thickness of water layer formed by all water in a certain
169 soil layer, which is expressed by formula as follows:



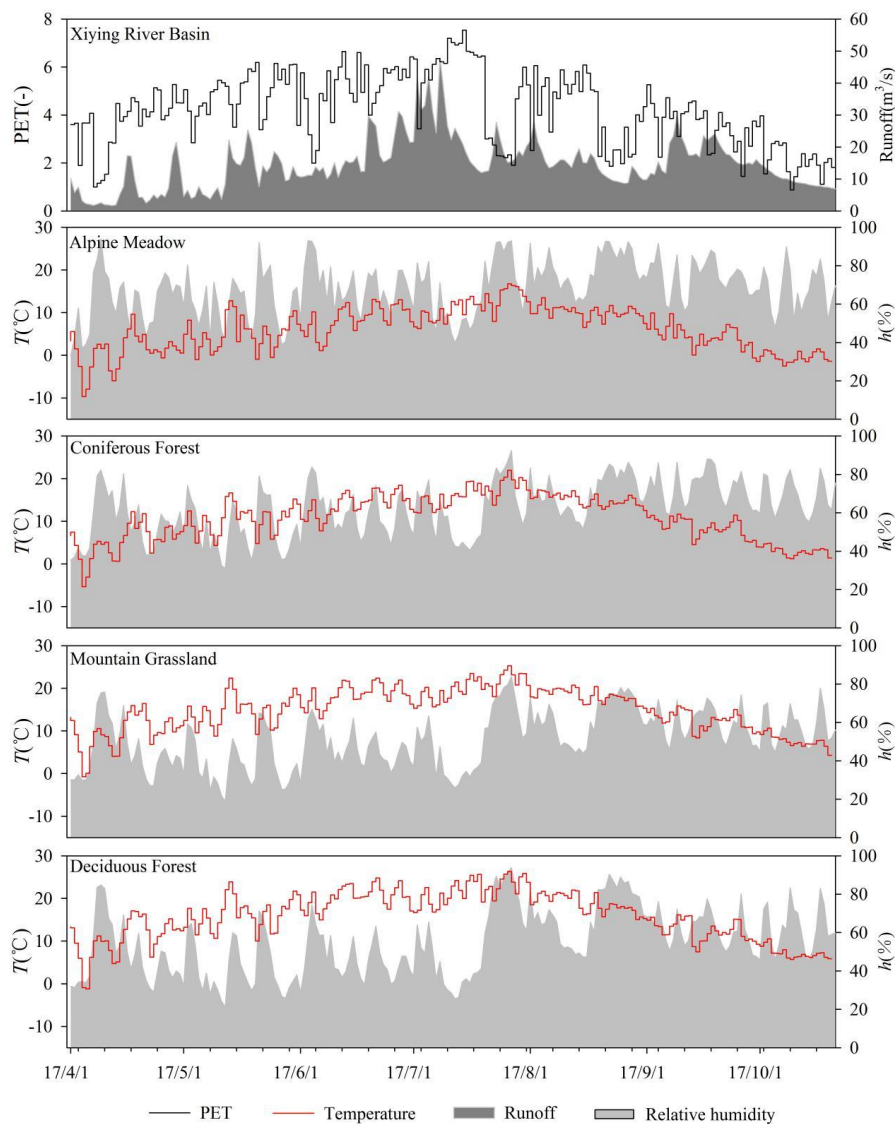
$$S = R \times W \times H \times 10 \quad (4)$$

170 where S is soil water storage in a certain thickness layer (mm), R is soil bulk density
171 (g cm^{-3}), H is soil thickness (cm), and W is soil weight moisture content in a certain
172 thickness layer.

173 **4. Results and analysis**

174 **4.1 Hydrological climate**

175 PET and runoff are important indicators to reflect the dry-wet conditions of river
176 basins. During the study period (April-October), the potential evapotranspiration was
177 872.8 mm, and the daily evapotranspiration ranged from 7.5 mm (July 14) to 0.9 mm
178 (October 9) in Xiyang River Basin, showing a fluctuating increase and decrease trend
179 around July. PET in April-July was higher than that in August-October. The input of
180 summer precipitation and ice-snow melt water masked the strong evaporation,
181 changed the negative correlation between runoff and PET, and led to the changing
182 trend of runoff similar to PET. Total runoff during the observation period was $3.1 \times$
183 10^9 m, accounting for 89% of the total annual runoff. The variation range of daily
184 runoff was 286,848 m^3 (April 17) to 6,125,760 m^3 (July 13). Generally speaking,
185 during the study period, the basin was drier before July than after July (Fig.2).



186

187 **Fig. 2** Climatic and hydrological conditions of Xiyi River basin and its vegetation
188 zones

189 To explore the differences in the natural environment in different vegetation
190 zones, air temperature, atmospheric humidity, and precipitation were used to indicate
191 each research site's heat and moisture conditions. Hilltop is a typical Alpine Meadow
192 zone, with a daily average temperature of 6.1°C, ranging from -9.7°C (April 5) to



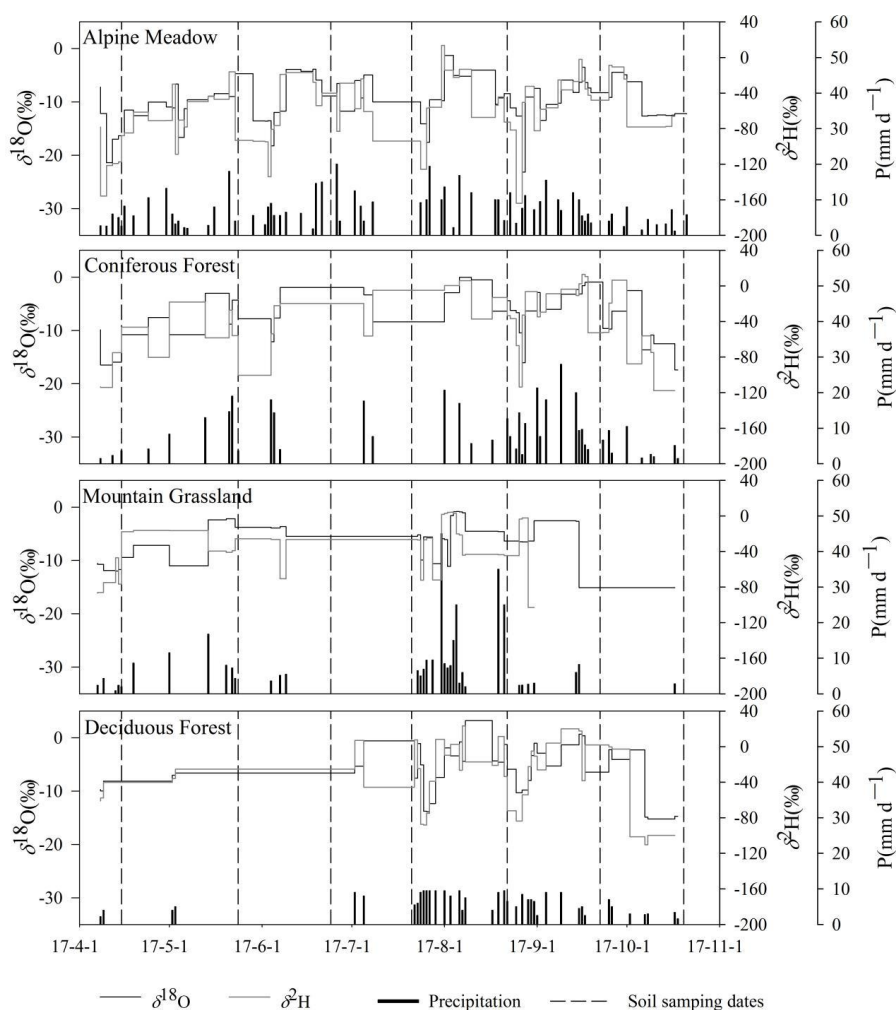
193 16.8°C (July 27). The average daily humidity was 68.2%, with little difference in
194 different periods. There were 72 precipitations in the vegetation zone during the
195 observation period, with total precipitation of 534.3 mm, which was relatively evenly
196 distributed in each month. In the Coniferous Forest zone, the average daily
197 temperature during the study period was 10.9°C, ranging from -5.4°C (April 5) to
198 22.0°C (July 27). The average daily humidity was 62.5%, and the precipitation was
199 400.6 mm, mainly concentrated from early August to late September. Close to the
200 foothills is the Mountain Grassland zone, with a daily average temperature of 14.9°C,
201 ranging from -0.7°C (April 5) to 25.3°C (July 27). The average daily humidity was
202 51.1%, and the precipitation of the vegetation zone during the observation period was
203 327.2 mm, mainly from late July to mid-August. During the observation period, the
204 average daily temperature at the Deciduous Forest zone was 15.8°C, ranging from
205 -1.2°C (April 6) to 26.3°C (July 27). The average daily humidity was 54.7%, and the
206 total precipitation was 250.6 mm, which was concentrated in the month from late July
207 to late August. To sum up, the heat of the four vegetation zones was
208 AM<CF<MG<DF and the moisture condition was AM > CF > MG > DF (Fig. 2 and
209 Fig. 3).

210 **4.2 Time variation of water stable isotopes in different vegetation zones**

211 Influenced by different water sources and complex weather conditions in the
212 precipitation process, the isotopic composition of precipitation in four vegetation
213 zones was obviously different during the study period. The mean values of $\delta^2\text{H}$ and
214 $\delta^{18}\text{O}$ in Alpine Meadow were $-73.1\text{‰}\pm 36.3\text{‰}$ ($-163.9\text{‰}\sim 13.7\text{‰}$) and $-10.0\text{‰}\pm 4.3\text{‰}$
215 ($-23.1\text{‰}\sim -1.3\text{‰}$), respectively. The average values of $\delta^2\text{H}$ and $\delta^{18}\text{O}$ of Coniferous
216 Forest were $-42.0\text{‰}\pm 37.2\text{‰}$ ($-117.8\text{‰}\sim 13.0\text{‰}$) and $-7.1\text{‰}\pm 4.7\text{‰}$ ($-17.4\text{‰}\sim -0.1\text{‰}$),
217 respectively. The average values of $\delta^2\text{H}$ and $\delta^{18}\text{O}$ of Mountain Grassland were
218 $-37.4\text{‰}\pm 30.5\text{‰}$ ($-103.1\text{‰}\sim 4.2\text{‰}$) and $-5.9\text{‰}\pm 3.9\text{‰}$ ($-15.1\text{‰}\sim -0.9\text{‰}$), respectively.
219 The average values of $\delta^2\text{H}$ and $\delta^{18}\text{O}$ of Deciduous Forest were $-31.8\text{‰}\pm 42.8\text{‰}$
220 ($-110.2\text{‰}\sim 23.2\text{‰}$) and $-5.8\text{‰}\pm 5.5\text{‰}$ ($-15.2\text{‰}\sim 3.2\text{‰}$), respectively. The maximum
221 isotopic values of the four vegetation zones appeared on August 4 (Alpine Meadow),



222 August 10 (Coniferous Forest), August 7 (Mountain Grassland) and August 13
223 (Deciduous Forest), respectively, which were 7 days, 13 days, 10 days and 16 days
224 behind the local maximum temperature. In addition, the atmospheric precipitation
225 isotopes of the four vegetation zones had similar time variations: from April to August,
226 the fluctuation of $\delta^2\text{H}$ and $\delta^{18}\text{O}$ increased, reached the maximum in mid-August, and
227 then gradually decreased (Fig. 3).



228

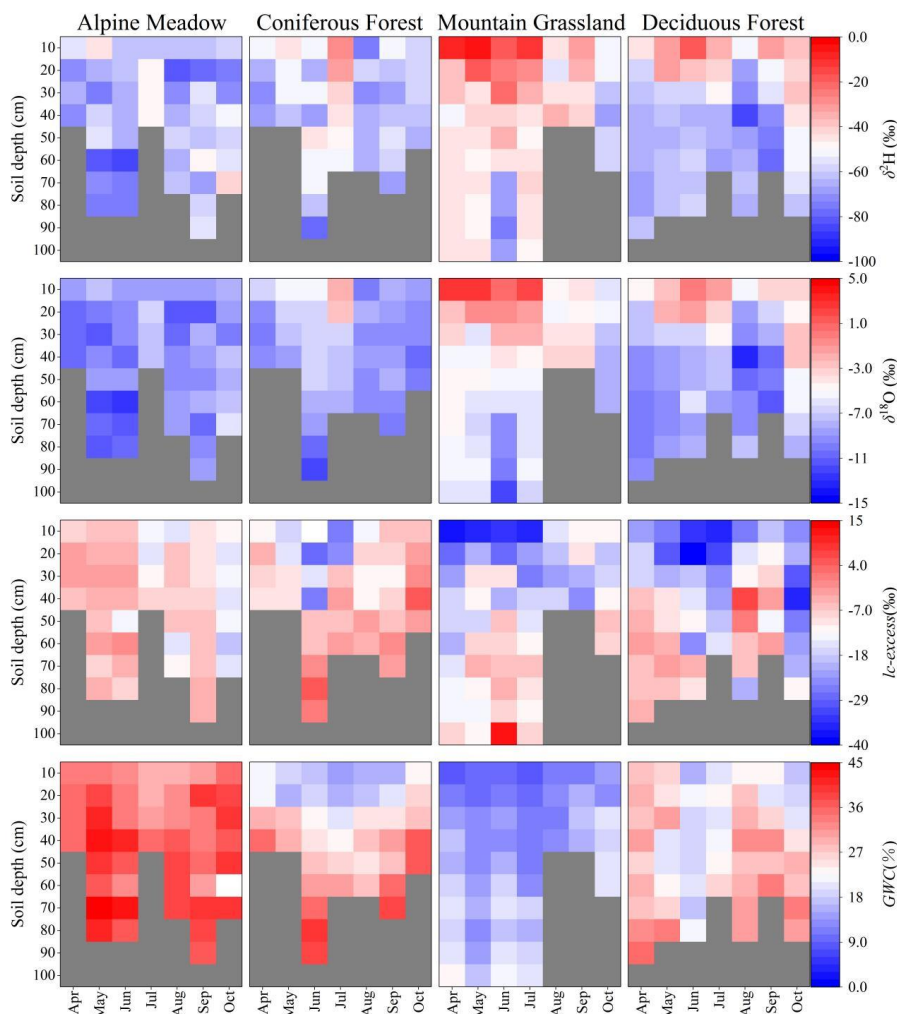
229 **Fig. 3** Time series of rainfall and isotope characteristics in different vegetation
230 zones in Xiyang River Basin, with dotted lines indicating the date of soil water

231

sampling



232 The monthly variation of soil water isotope records the signal of precipitation
233 input and evaporation. The low temperature environment of Alpine Meadow and
234 abundant and uniform precipitation events made the monthly mean values of $\delta^2\text{H}$ and
235 $\delta^{18}\text{O}$ change little and were most depleted than other vegetation belts. Despite this,
236 SWlc-excess of most samples in this station was still negative, and there were
237 different degrees of evaporation in the process of precipitation penetrating the soil and
238 mixing with original pore water, among which evaporation fractionation was stronger
239 in July (-11.5‰, lc-excess) and October (-14.9‰, lc-excess). Evaporation
240 fractionation of soil water isotopes in Coniferous Forests was more intense. Soil water
241 isotopes of Coniferous Forest gradually changed seasonally. From April to July,
242 precipitation was scarce, the temperature rose, and the isotopes of soil water was
243 gradually enriched on the surface, reaching the peak value of the observation period in
244 July (-29.5‰, $\delta^2\text{H}$; -2.1‰, $\delta^{18}\text{O}$), and continuous rainfall input from late July to
245 mid-August resulted in soil water isotopes depletion. SWlc-excess was an obvious
246 fractionation signal opposite to the trend of isotope change, reaching the lowest value
247 (-26.3‰) in the sampling period in July, and the change of air temperature and
248 precipitation controlled the evaporation intensity. From April to July, the isotopic
249 value of surface soil water in Mountain Grassland was higher ($\delta^{18}\text{O}$ was greater than
250 zero), and SWlc-excess was lower than -30‰. During this period, evaporation and
251 fractionation of shallow soil water were intense. Similar to the Coniferous Forest, the
252 input of heavy precipitation from late July to mid-August led to the depletion of soil
253 water isotopes. There was only sporadic rainfall in Deciduous Forest from April to
254 July, and the soil water isotopes were gradually enriched on the surface and reached
255 its peak in June when there was no rainfall event (-18.2‰, $\delta^2\text{H}$; 0.2‰, $\delta^{18}\text{O}$), and
256 then became depleted. In addition, due to the influence of Xiyang Reservoir and
257 vegetation coverage, the isotopic enrichment degree of soil water in this vegetation
258 zone was lower than that in Mountain Grassland. As the most intuitive form of water
259 change, GWC (gravimetric water content) was always at a low value in July, when the
260 evaporation was the strongest, and it was most obvious in shallow soil (Fig. 4).



261

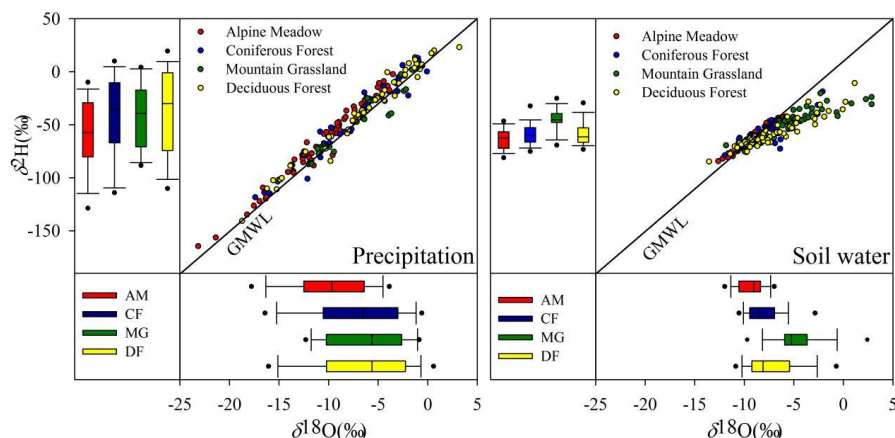
262 **Fig. 4** Heat map of soil depth profile of $\delta^2\text{H}$, $\delta^{18}\text{O}$, $lc\text{-excess}$ and GWC in different
263 vegetation zones, and the layer lacking measurement is indicated by deep color

264 4.3 Spatial variation of water stable isotopes in different vegetation zones

265 Isotope data of precipitation and soil water obtained from different vegetation
266 zones were shown in the double isotope diagram (Fig. 5). In the Alpine Meadow
267 observation station, the secondary evaporation was low due to low temperature, low
268 cloud bottom height, and low air saturated water vapor loss. In addition, the monsoon
269 caused strong convective precipitation at the station. Therefore, the slope (8.35) and
270 intercept (23) of LMWL were higher than GMWL. The slope of LMWL in the other



271 three vegetation zones was lower than GMWL, and gradually decreased with altitude
272 decrease. This was mainly because in arid areas, with the decrease of altitude, the
273 secondary evaporation under clouds was strengthened, and the strong evaporation will
274 lead to the decrease of intercept. The $\delta^2\text{H}$ and $\delta^{18}\text{O}$ of soil water in each vegetation
275 zone mostly fall in the lower right of LMWL, indicating that atmospheric
276 precipitation was the main supply source of soil water, subject to different degrees of
277 soil water evaporation. With the decrease of altitude, the soil water evaporation
278 became stronger and stronger, except soil in Deciduous Forest. On the one hand, the
279 vegetation coverage of this site was higher. On the other hand, Xiying Reservoir
280 enhanced the regional air humidity and slowed down the local water vapor circulation
281 driving force.



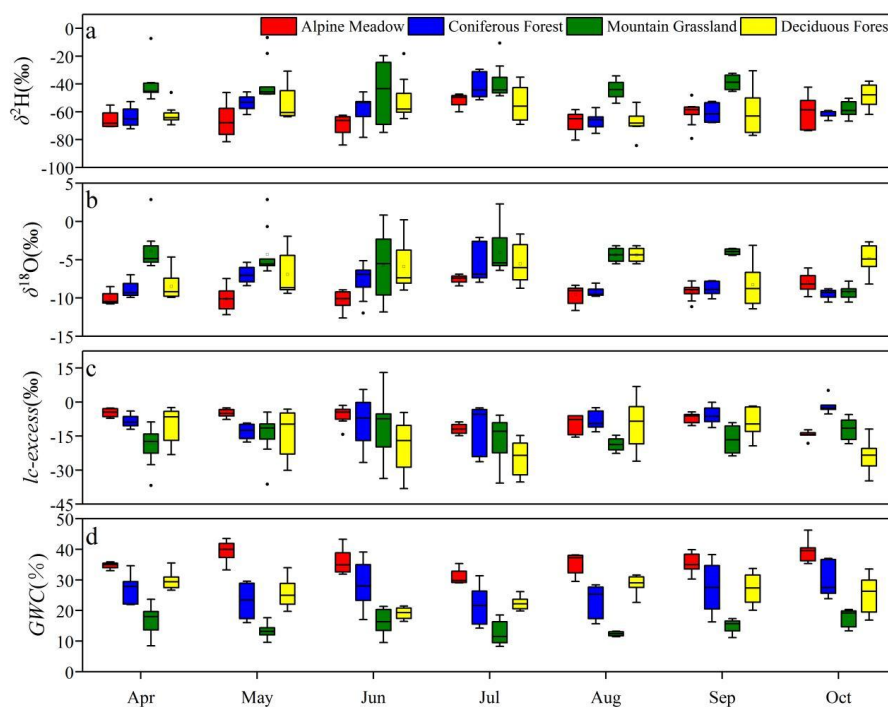
282
283 **Fig. 5** Double isotope diagram of precipitation (left) and soil water (right) isotope
284 data of four vegetation zones. In the box plots, the box represents 25%-75%
285 percentile, the line in the box represents median (50th percentile), the required line
286 indicates 90th and 10th percentile, and the point indicates the 95th and 5th
287 percentile.

288 During the study period, compared with soil water in Alpine Meadow and
289 Coniferous Forest, the isotopic value of soil water in Mountain Grassland and
290 Deciduous Forest was relatively enriched, the lc-excess was smaller and deeper into
291 the middle and lower soil layers, and the GWC was relatively low. Because of the



292 difference in vegetation types and the influence of reservoirs, this change did not have
293 the elevation effect completely. Although the elevation was low, the soil water of
294 Deciduous Forest had more depleted isotopic characteristics and higher soil moisture
295 than Mountain Grassland in most samples (Fig. 4).

296 Soil profiles obtained from different vegetation zones can reflect the evaporation
297 signals of water. Low temperature natural environment made Alpine Meadow soil less
298 affected by dynamic fractionation ($l_c\text{-excess} > -20\text{‰}$), and GWC was at a high value
299 ($GWC > 25\%$) during the whole study period. The surface soil water of Coniferous
300 Forest was easily affected by climate, and had higher isotopic composition (-29.5‰ ,
301 $\delta^2\text{H}$; -2.1‰ , $\delta^2\text{H}$) and lower $l_c\text{-excess}$ (-26.3). With the increase of soil depth, the
302 fractionation signal gradually weakened, $\delta^2\text{H}$ and $\delta^{18}\text{O}$ became depleted, and soil
303 water content gradually increased. Isotopes of soil water in Mountain Grassland and
304 Deciduous Forest were enriched in surface soil layer due to fractionation. Especially
305 in the Mountain Grassland, the average values of $\delta^2\text{H}$ and $\delta^{18}\text{O}$ in 0-10cm soil layer
306 were as high as -24.4‰ and -1.2‰ , respectively, and $SWl_c\text{-excess}$ was lower than
307 25% , even close to 40% in some samples. Evaporation signal can easily penetrate
308 deep soil, which made the GWC value of all sampling activities at this site lower than
309 20% (Fig.6).



310
311 **Fig. 6** the differences of $\delta^2\text{H}$, $\delta^{18}\text{O}$, lc-excess and GWC in different vegetation zones
312 in each sampling

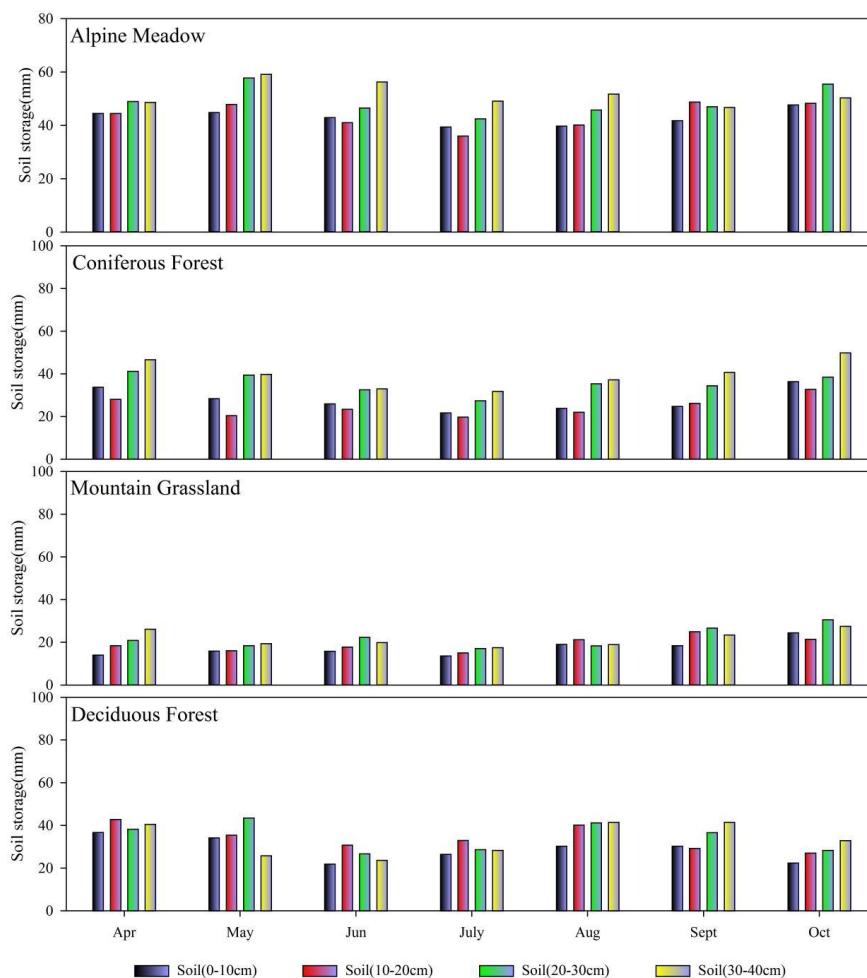
313 5. Discussion

314 5.1 Soil water storage capacity of different vegetation belts in arid headwaters 315 area

316 As the temperature decreases rapidly with the increase of height, the
317 precipitation and humidity increase to a certain extent, and the vegetation shows a
318 strip-like alternation approximately parallel to the contour line, forming zonal
319 vegetation with obvious differentiation (Yin et al., 2020). The dry-wet conditions of
320 different vegetation zones restrict the soil water storage capacity in the basin. The
321 rainfall decreased, the temperature rose, the groundwater level dropped and the soil
322 water storage capacity was weak during the replacement of vegetation zones to low
323 altitudes (Coussement et al., 2018; Kleine et al., 2020). The soil water storage
324 capacity of Alpine Meadow with low temperature and rainy weather was obviously
325 higher than that of other vegetation zones. The soil water storage capacity (0-40 cm)



326 of each sample during the study period exceeded 165 mm, with little difference
327 between months and no obvious change between months. With the decrease of
328 altitude, the monthly difference of dry-wet conditions in each vegetation zone
329 gradually became obvious. With the increase of summer temperature, the environment
330 became dry, and the soil water storage capacity weakened (Sprenger et al., 2017). The
331 soil water storage capacity of Coniferous Forest began to decrease in April, and the
332 water storage capacity of 0-40 cm reached the minimum value (101.2 mm) in July.
333 The change in temperature and precipitation was the main reason for the monthly
334 difference (Dubber and Werner, 2019). Although there was a certain water storage
335 capacity in Coniferous Forest with some water transpiration loss, the soil water
336 storage capacity in this vegetation zone was not strong. The water storage capacity of
337 Mountain Grassland soil was lower than that of other vegetation zones. The
338 continuous dry and warm weather in spring and summer led to the water storage
339 capacity of 0-40 cm soil being lower than that of 100 mm every month. Particularly,
340 drought stress leads to insufficient soil moisture, making it difficult to maintain plant
341 demand, resulting in sparse vegetation and large-scale exposed surface soil, which
342 further accelerates surface water loss. The continuous rainfall from the end of July
343 prevented the further development of drought, and the input of water gradually
344 restored the soil water storage capacity (Kleine et al., 2020). Deciduous Forest had
345 similar hydrothermal conditions with Mountain Grassland, but the soil porosity of
346 forest land is obviously larger than that of barren land, and its permeability was better
347 than that of barren land. Rainwater was sent to the ground through roots and turned
348 into groundwater. Forest was a reservoir with strong water storage and soil
349 conservation capacity (Sprenger et al., 2019). The water storage capacity of 0-40 cm
350 soil sampled every time in Deciduous Forest was higher than that in 100 mm soil. In
351 addition, the water content of 0-40 cm soil layer in each vegetation zone increased
352 with the deepening of the soil layer, and the water storage capacity of surface soil was
353 weak. The difference of soil properties will also lead to more water stored in the
354 middle and lower soil with higher clay content (Heinrich et al., 2019) (Fig. 7).



355

356 **Fig. 7** Monthly variation of soil water storage in 0-40cm soil layer of different
357 vegetation zones

358 **5.2 "Memory" effect of isotope signals on soil water migration in different**
359 **vegetation zones**

360 Isotopic signals can evaluate the effects of dry-wet conditions in different
361 vegetation zones on soil water transport. After rainfall, the variability of isotope signal
362 at a certain soil depth can identify the seepage way of water (Peralta-Tapia et al.,
363 2015). During the study period, the soils of Alpine Meadow and Coniferous Forest
364 were seasonally frozen and thawed all the year-round, and the isotope difference of



365 soil isotope profile was small, and precipitation mainly penetrated into the soil in the
366 form of plug flow. Preferential infiltration showed high variability of isotopic signal
367 (Brodersen et al., 2000), and rainwater in Mountain Grassland and Deciduous
368 Forest flowed into deep soil rapidly through soil matrix through exposed soil fissures
369 and roots. Water movement and mixing in the unsaturated zone can be observed in the
370 space-time variation of isotope within 1 meter of the soil profile. In addition, the
371 dynamic changes of $\delta^{13}C$ -excess in soil profiles of different vegetation zones reflected
372 the evaporation signals caused by drought during the study period. Particularly in low
373 altitude areas, soil evaporation in spring and summer and insufficient precipitation
374 during drought were the main driving forces leading to isotopic enrichment in the
375 surface soil of Mountain Grassland and Deciduous Forest (Kleine et al., 2020).
376 Alpine Meadow and Coniferous Forest zone were rich in rainfall. After a short period
377 of weak evaporation, the soil will be rewetted by the next rainfall. The Mountain
378 Grassland and Deciduous Forest zone had only sporadic precipitation from mid-May
379 to late July, and the soil moisture evaporates rapidly. With the decrease of air
380 temperature and the occurrence of continuous precipitation after July, the soil was
381 re-wetted after two months of drought, and both vegetation zones showed the
382 replacement and mixing of soil water isotope and precipitation. There were
383 commonalities in soil moisture changes in different vegetation zones characterized by
384 more enriched isotopes, stronger evaporation signal, and lower moisture content in
385 shallow soil. With the increase of soil depth, isotope was gradually depleted, and
386 evaporation signal was gradually weakened until it disappeared. The evolution of
387 isotopes, $\delta^{13}C$ -excess, and GWC in unsaturated soil showed the differences among
388 different vegetation zones. From high altitude to low altitude, the isotopic value of the
389 surface gradually enriched and the evaporation signal increased. The low vegetation
390 coverage on the Mountain Grassland made the evaporation front penetrate deeper into
391 the soil layer, and there was still an obvious evaporation signal below 70 cm of the
392 surface (Fig. 4). The results showed that the storage of soil and groundwater in this
393 area was seriously insufficient, which reflected the incomplete rewetting of the basin



394 at the end of the study. In addition, lower soil water storage capacity will make the
395 remaining soil water have a stronger Rayleigh fractionation effect (Zimmermann et al.,
396 1966; Barnes and Allison, 1988). Similar evaporation signals have been found in the
397 Mediterranean and arid climate regions (Sprenger et al., 2016b; McCutcheon et al.,
398 2017). Evaporation signal only exists in the surface soil in humid areas, and there
399 is no significant difference between $\delta^{18}O$ -excess and 0 in the soil layer below 20cm
400 (Sprenger et al., 2017). We observed the isotopic drought signal ($\delta^{18}O$ -excess) and the
401 "memory" effect of soil rewetting caused by precipitation input and mixing in
402 different vegetation zones during the whole study period. The continuous separation
403 of soil moisture reflected different soil and climate attributes and formed different
404 hydrological paths.

405 **5.3 Understanding of watershed runoff and water resources management**

406 Climate warming and the spatiotemporal imbalance of water resources interfere
407 with the ecological-water balance of different vegetation zones in inland river source
408 areas (Liu et al., 2015). The growth of plants mainly depends on the water stored in
409 shallow soil layer (Amin et al., 2019). Drought reduces the water storage of soil,
410 inhibits the growth of plants and leads to the decrease of stomatal conductance of
411 plants, finally causing plant death due to lack of water or carbon (Li et al., 2020). In
412 recent years, dry and hot summers have become more common. Understanding the
413 soil water and hydrological process of the unsaturated zone in basin areas using the
414 stable isotopic method is very important for formulating ecological restoration and
415 water resources management strategies in vulnerable areas under the background of
416 climate warming (Kleine et al., 2020). The management of watershed runoff and
417 water resources in different vegetation zones should be based on local hydrological
418 and climatic conditions, and the influence of human activities should also be
419 considered. The Alpine Meadow vegetation zone has steep terrain. Abundant
420 precipitation and glacier snow provide sufficient water for unsaturated zone soil and
421 easily form slope runoff when rainfall intensity or snowmelt intensity exceeds the
422 infiltration capacity of ground soil. Some of the infiltration water is incompletely lost,



423 which becomes underground runoff, so runoff includes surface and underground
424 runoff. With the global warming in recent years, despite the increase of runoff, the
425 glacier area is shrinking, the ice and snow reserves are decreasing, and regional
426 climate regulation is weakened. In addition, the waste from mining activities will
427 pollute glaciers and even lead to the deterioration of water quality in the process of
428 runoff formed by rainfall and melting water of ice and snow. As a natural reservoir,
429 although the transpiration of plants is strong in the drought period, the soil water
430 storage capacity of the forest is still higher than that of other vegetation-covered soils
431 under the same climate conditions (Sprenger et al., 2019). The Coniferous Forest belt
432 is located on the mountainside, with a large slope on the ground. The continuous
433 heavy precipitation from late summer will form surface runoff and flow into Xiyang
434 River, and some water will seep into the soil layer to supply underground runoff.
435 There is little rainfall in the Deciduous Forest zone, and the terrain of this vegetation
436 zone is gentle. After rainfall reaches the ground, it is not easy to form slope runoff,
437 but easy to seep into the soil to replenish groundwater. In the arid period of Mountain
438 Grassland, the evaporation is strong, the water storage is less, and the groundwater is
439 buried deeply. After one rainfall, the water storage in the basin is not saturated, and all
440 the infiltration water is lost, making it difficult to form underground runoff. Only
441 when only a few rainfall intensity is greater than infiltration intensity, the
442 over-infiltration rain will occur, forming surface runoff. The soil moisture content in
443 this region is extremely low, and the growth of plants is inhibited, resulting in the
444 unsustainability of ecosystem services and agricultural and pastoral land. In order to
445 effectively improve and manage water resources in arid headwaters areas, it is
446 necessary to explore the heterogeneity among different vegetation zones and deeply
447 understand the runoff generation mechanism of different vegetation zones in
448 watershed runoff generation areas. According to the current situation of climate,
449 hydrology, and social economy in the basin, scientific and reasonable management
450 policies should be formulated according to local conditions for different
451 ecological-hydrological contradictions and extended to more areas.



452 **6. Conclusion**

453 This work provides further insights into the movement and mixing of soil water
454 in different vegetation zones in arid headwaters areas. Dry-wet conditions were the
455 key factors that restrict soil water storage capacity in different vegetation zones.
456 Rainfall decreased, temperature rose, groundwater level dropped, and soil water
457 storage capacity weakened in the vegetation zone change to low altitude. The water
458 storage capacity of the surface soil of each vegetation zone was weak, and more water
459 was stored in the middle and lower soil with higher clay content. During the study
460 period, the dynamic changes of $\delta^{18}O$ -excess in soil profiles of different vegetation zones
461 reflected the evaporation signals caused by drought. Soil evaporation in spring and
462 summer and insufficient precipitation during drought were the main driving forces
463 leading to $\delta^{18}O$ enrichment in surface soil. In low altitude vegetation zone, the
464 high temperature made evaporation front penetrate deeper into soil layer, and there
465 was still obvious evaporation signal below 70 cm of the surface. Soil water isotopes
466 and GWC record the process of soil rewetting caused by precipitation input and
467 mixing. Alpine Meadow and Coniferous Forest zones were rich in rainfall. After a
468 short period of weak evaporation, the soil will be rewetted by the next rainfall. There
469 was only sporadic precipitation in Mountainous Grassland and Deciduous Forest belt
470 from mid-May to late July. After July, the drop in temperature and continuous
471 precipitation made the soil wet again after two months of drought. The Mountain
472 Grassland and Deciduous Forest zone had only sporadic precipitation from mid-May
473 to late July. With the decrease of air temperature and continuous precipitation after
474 July, the soil was re-wetted after two months of drought. In addition, the Alpine
475 Meadow and Coniferous Forest zones had a steep slope and humid climate, which
476 was easy to form surface runoff and underground runoff in the rainy season and ice
477 and snow melting period. Low-altitude vegetation zone with flat terrain had dry
478 climate and scarce precipitation, and part of the water seeped into the middle and
479 lower layers of soil to accumulate or replenish groundwater, so it wasn't easy to form
480 slope flow. This research are helpful to understand the hydrological process of



481 different vegetation areas, and give managers to formulate scientific and reasonable
482 water resources, animal husbandry and mining area management policy decision
483 support.

484 **Reference**

- 485 Allen, R. G., Pereira, L. S., Raes, D., & Smith, M. (1998). Crop evapotranspiration-Guidelines for
486 computing crop water requirements-FAO Irrigation and drainage paper 56. *Fao,*
487 *Rome, 300(9)*, D05109.
- 488 Amin, A., Zuecco, G., Geris, J., Schwendenmann, L., McDonnell, J. J., Borga, M., & Penna, D.
489 (2020). Depth distribution of soil water sourced by plants at the global scale: A new direct
490 inference approach. *Ecohydrology, 13(2)*, e2177.
- 491 Barbeta, A., Mejía - Chang, M., Ogaya, R., Voltas, J., Dawson, T. E., & Peñuelas, J. (2015). The
492 combined effects of a long - term experimental drought and an extreme drought on the use of
493 plant - water sources in a Mediterranean forest. *Global change biology, 21(3)*, 1213-1225.
- 494 Barnes, C. J., & Allison, G. B. (1988). Tracing of water movement in the unsaturated zone using
495 stable isotopes of hydrogen and oxygen. *Journal of Hydrology, 100(1-3)*, 143-176.
- 496 Brodersen, C., Pohl, S., Lindenlaub, M., Leibundgut, C., & Wilpert, K. V. (2000). Influence of
497 vegetation structure on isotope content of throughfall and soil water. *Hydrological*
498 *Processes, 14(8)*, 1439-1448.
- 499 Brooks, J. R., Barnard, H. R., Coulombe, R., & McDonnell, J. J. (2010). Ecohydrologic separation
500 of water between trees and streams in a Mediterranean climate. *Nature Geoscience, 3(2)*,
501 100-104.
- 502 Cheng, L., Liu, W., Li, Z., & Chen, J. (2014). Study of soil water movement and groundwater
503 recharge for the loess tableland using environmental tracers. *Transactions of the*
504 *ASABE, 57(1)*, 23-30.
- 505 Coussement, T., Maloteau, S., Pardon, P., Artru, S., Ridley, S., Javaux, M., & Garré, S. (2018). A
506 tree-bordered field as a surrogate for agroforestry in temperate regions: Where does the water
507 go?. *Agricultural Water Management, 210*, 198-207.
- 508 Cui, Y., Ma, J., Sun, W., Sun, J., & Duan, Z. (2015). A preliminary study of water use strategy of
509 desert plants in Dunhuang, China. *Journal of Arid Land, 7(1)*, 73-81.



- 510 Douinot, A., Tetzlaff, D., Maneta, M., Kuppel, S., Schulte - Bisping, H., & Soulsby, C. (2019).
511 Ecohydrological modelling with Ech2O - iso to quantify forest and grassland effects on
512 water partitioning and flux ages. *Hydrological Processes*, 33(16), 2174-2191.
- 513 Dubbert, M., & Werner, C. (2019). Water fluxes mediated by vegetation: emerging isotopic
514 insights at the soil and atmosphere interfaces. *New Phytologist*, 221(4), 1754-1763.
- 515 Dubbert, M., Cuntz, M., Piayda, A., Maguás, C., & Werner, C. (2013). Partitioning
516 evapotranspiration—Testing the Craig and Gordon model with field measurements of oxygen
517 isotope ratios of evaporative fluxes. *Journal of Hydrology*, 496, 142-153.
- 518 Ferretti, D. F., Pendall, E., Morgan, J. A., Nelson, J. A., Lecain, D., & Mosier, A. R. (2003).
519 Partitioning evapotranspiration fluxes from a Colorado grassland using stable isotopes:
520 Seasonal variations and ecosystem implications of elevated atmospheric CO₂. *Plant and
521 Soil*, 254(2), 291-303.
- 522 Grant, G. E., & Dietrich, W. E. (2017). The frontier beneath our feet. *Water Resources
523 Research*, 53(4), 2605-2609.
- 524 Heinrich, I., Balanzategui, D., Bens, O., Blume, T., Brauer, A., Dietze, E., ... & Wille, C. (2019).
525 Regionale Auswirkungen des Globalen Wandels: Der Extremsommer 2018 in
526 Nordostdeutschland. *System Erde*, 9(1), 38-47.
- 527 Hsieh, J. C., Chadwick, O. A., Kelly, E. F., & Savin, S. M. (1998). Oxygen isotopic composition
528 of soil water: quantifying evaporation and transpiration. *Geoderma*, 82(1-3), 269-293.
- 529 Kleine, L., Tetzlaff, D., Smith, A., Wang, H., & Soulsby, C. (2020). Using water stable isotopes to
530 understand evaporation, moisture stress, and re-wetting in catchment forest and grassland
531 soils of the summer drought of 2018. *Hydrology and Earth System Sciences*, 24(7),
532 3737-3752.
- 533 Koeniger, P., Gaj, M., Beyer, M., & Himmelsbach, T. (2016). Review on soil water
534 isotope - based groundwater recharge estimations. *Hydrological Processes*, 30(16),
535 2817-2834.
- 536 Landwehr, J. M., & Coplen, T. B. (2006, February). Line-conditioned excess: a new method for
537 characterizing stable hydrogen and oxygen isotope ratios in hydrologic systems.



- 538 In International conference on isotopes in environmental studies (pp. 132-135). Vienna:
539 IAEA.
- 540 Landwehr, J. M., Coplen, T. B., & Stewart, D. W. (2014). Spatial, seasonal, and source variability
541 in the stable oxygen and hydrogen isotopic composition of tap waters throughout the
542 USA. *Hydrological Processes*, 28(21), 5382-5422.
- 543 Li, X., Piao, S., Wang, K., Wang, X., Wang, T., Ciais, P., ... & Peñuelas, J. (2020). Temporal
544 trade-off between gymnosperm resistance and resilience increases forest sensitivity to
545 extreme drought. *Nature Ecology & Evolution*, 4(8), 1075-1083.
- 546 Liu, Y., Liu, F., Xu, Z., Zhang, J., Wang, L., & An, S. (2015). Variations of soil water isotopes and
547 effective contribution times of precipitation and throughfall to alpine soil water, in Wolong
548 Nature Reserve, China. *Catena*, 126, 201-208.
- 549 Lupwayi, N. Z., Rice, W. A., & Clayton, G. W. (1998). Soil microbial diversity and community
550 structure under wheat as influenced by tillage and crop rotation. *Soil Biology and
551 Biochemistry*, 30(13), 1733-1741.
- 552 McCutcheon, R. J., McNamara, J. P., Kohn, M. J., & Evans, S. L. (2017). An evaluation of the
553 ecohydrological separation hypothesis in a semiarid catchment. *Hydrological
554 processes*, 31(4), 783-799.
- 555 Penna, D., Hopp, L., Scandellari, F., Allen, S. T., Benettin, P., Beyer, M., ... & Kirchner, J. W.
556 (2018). Ideas and perspectives: Tracing terrestrial ecosystem water fluxes using hydrogen and
557 oxygen stable isotopes—challenges and opportunities from an interdisciplinary
558 perspective. *Biogeosciences*, 15(21), 6399-6415.
- 559 Peralta - Tapia, A., Sponseller, R. A., Tetzlaff, D., Soulsby, C., & Laudon, H. (2015). Connecting
560 precipitation inputs and soil flow pathways to stream water in contrasting boreal
561 catchments. *Hydrological Processes*, 29(16), 3546-3555.
- 562 Rothfuss, Y., & Javaux, M. (2017). Reviews and syntheses: Isotopic approaches to quantify root
563 water uptake: a review and comparison of methods. *Biogeosciences*, 14(8), 2199-2224.
- 564 Seiler, K. P., Von Loewenstern, S., & Schneider, S. (2002). Matrix and bypass-flow in quaternary
565 and tertiary sediments of agricultural areas in south Germany. *Geoderma*, 105(3-4), 299-306.



- 566 Simonin, K. A., Link, P., Rempe, D., Miller, S., Oshun, J., Bode, C., ... & Dawson, T. E. (2014).
567 Vegetation induced changes in the stable isotope composition of near surface
568 humidity. *Ecohydrology*, 7(3), 936-949.
- 569 Sprenger, M., Erhardt, M., Riedel, M., & Weiler, M. (2016a). Historical tracking of nitrate in
570 contrasting vineyards using water isotopes and nitrate depth profiles. *Agriculture, Ecosystems
571 & Environment*, 222, 185-192.
- 572 Sprenger, M., Leister, H., Gimbel, K., & Weiler, M. (2016b). Illuminating hydrological processes
573 at the soil - vegetation - atmosphere interface with water stable isotopes. *Reviews of
574 Geophysics*, 54(3), 674-704.
- 575 Sprenger, M., Tetzlaff, D., & Soulsby, C. (2017). Soil water stable isotopes reveal evaporation
576 dynamics at the soil-plant-atmosphere interface of the critical zone. *Hydrology and Earth
577 System Sciences*, 21(7), 3839-3858.
- 578 Sprenger, M., Llorens, P., Cayuela, C., Gallart, F., & Latron, J. (2019). Mechanisms of
579 consistently disjunct soil water pools over (pore) space and time. *Hydrology and Earth
580 System Sciences*, 23(6), 2751-2762.
- 581 Stumpp, C., Stichler, W., Kandolf, M., & Šimůnek, J. (2012). Effects of land cover and
582 fertilization method on water flow and solute transport in five lysimeters: A long - term study
583 using stable water isotopes. *Vadose Zone Journal*, 11(1).
- 584 Tang, K., & Feng, X. (2001). The effect of soil hydrology on the oxygen and hydrogen isotopic
585 compositions of plants' source water. *Earth and Planetary Science Letters*, 185(3-4), 355-367.
- 586 Tetzlaff, D., Soulsby, C., Buttle, J., Capell, R., Carey, S. K., Laudon, H., ... & Shanley, J. (2013).
587 Catchments on the cusp? Structural and functional change in northern
588 ecohydrology. *Hydrological Processes*, 27(5), 766-774.
- 589 Wang, L., d'Odorico, P., Evans, J. P., Eldridge, D. J., McCabe, M. F., Caylor, K. K., & King, E. G.
590 (2012). Dryland ecohydrology and climate change: critical issues and technical
591 advances. *Hydrology and Earth System Sciences*, 16(8), 2585-2603.
- 592 Wenner, D. B., Ketcham, P. D., & Dowd, J. F. (1991). Stable isotopic composition of waters in a
593 small Piedmont watershed. In *Stable isotope geochemistry: a tribute to Samuel Epstein* (pp.
594 195-203).



- 595 Wookey, P. A., Aerts, R., Bardgett, R. D., Baptist, F., Bråthen, K. A., Cornelissen, J. H., ... &
596 Shaver, G. R. (2009). Ecosystem feedbacks and cascade processes: understanding their role
597 in the responses of Arctic and alpine ecosystems to environmental change. *Global Change*
598 *Biology*, 15(5), 1153-1172.
- 599 Xiao, W., Wei, Z., & Wen, X. (2018). Evapotranspiration partitioning at the ecosystem scale using
600 the stable isotope method—A review. *Agricultural and Forest Meteorology*, 263, 346-361.
- 601 Yin, L. , Dai, E. , Zheng, D. , Wang, Y. , & Tong, M. . (2020). What drives the vegetation
602 dynamics in the hengduan mountain region, southwest china: climate change or human
603 activity?. *Ecological Indicators*, 112, 106013.
- 604 Zhang, Y., Zhu, G., Ma, H., Yang, J., Pan, H., Guo, H., ... & Yong, L. (2019). Effects of Ecological
605 Water Conveyance on the Hydrochemistry of a Terminal Lake in an Inland River: A Case
606 Study of Qingtu Lake in the Shiyang River Basin. *Water*, 11(8), 1673.
- 607 Zimmermann, U., Münnich, K. O., Roether, W., Kreutz, W., Schubach, K., & Siegel, O. (1966).
608 Tracers determine movement of soil moisture and evapotranspiration. *Science*, 152(3720),
609 346-347.

610 **Acknowledgments**

611 This research was financially supported by the National Natural Science
612 Foundation of China (41661005, 41867030, 41971036). The authors much thank the
613 colleagues in the Northwest Normal University for their help in fieldwork, laboratory
614 analysis, data processing.

615 **Author Contribution statement**

616 Guofeng Zhu and Leilei Yong conceived the idea of the study; Yuanxiao Xu and
617 Qiaozhuo Wan analyzed the data; Zhigang Sun and Leilei Yong were responsible for
618 field sampling; Zhuanxia Zhang participated in the experiment; Lei Wang participated
619 in the drawing; Leilei Yong wrote the paper; Liyuan Sang and Yuwei Liu checked and
620 edited language. All authors discussed the results and revised the manuscript.

621 **Additional Information**

622 Competing Interests: The authors declare no competing interests.

623